



Fracture Morphology of Single-Lap Dissimilar Joints Between Thermoplastic Composite and AA5754-H111 with Laser Ablation Surface Pre-Treatment

Termoplastik Kompozit ve Lazer Uzaklaştırmalı Yüzey Ön İşlem Uygulanmış AA5754-H111 Arasındaki Bindirme Şeklinde Farklı Birleştirmelerin Kırılma Morfolojisi

Nahit Öztoprak* , Gökçe Mehmet Gençer 

Dokuz Eylül University, Department of Mechanical Engineering, İzmir, Türkiye

Abstract

Hot pressing is successfully proposed to bond metallic and polymeric materials as a direct-joining method to replace conventional assembly techniques. This article reports an experimental investigation on the failure mechanism analysis of single-lap joints (SLJs) subjected to tensile-shear loading. Al5754 alloy in H111 condition and long glass fiber reinforced-polypropylene (PP) composite are used as the adherends. In order to enhance the bond strength, laser processing is applied to the metal surface. A grid texture model by eight consecutive times scanning is utilized for the surface modification. After fabrication of the dissimilar joint, quasi-static mechanical performance of the metal-polymer hybrid structure is elucidated through tensile-shear testing. Thereafter, morphology of the fracture surfaces is evaluated by scanning electron microscopy (SEM). The experimental findings reveal that the laser surface texturing is proved to be an outstanding candidate for achieving strong joints through micro-interlocking in such metal/polymer multi-material connections. The ultimate force reaches the value of 1515.10 N after the 20 W laser surface pre-treatment.

Keywords: Single lap joints, Hot pressing, Laser ablation treatment, Fracture surface

Öz

Sıcak presleme geleneksel montaj tekniklerinin yerine doğrudan birleştirme yöntemi olarak metalik ve polimerik malzemeleri yapıştırmak için başarıyla önerilmektedir. Bu makale, çekme-kesme yüklemesine maruz kalan tek bindirmeli bağlantıların hasar mekanizması analizi üzerine deneysel bir araştırmayı bildirmektedir. Yapıştırılan malzemeler olarak H111 durumunda Al5754 alaşımı ve uzun cam elyaf takviyeli polipropilen (PP) kompozit kullanılmıştır. Bağlantı dayanımını arttırmak için metal yüzeye lazer işlemi uygulanmıştır. Yüzey modifikasyonu için art arda sekiz kez tarama ile bir ızgara doku modeli kullanılmıştır. Farklı bağlantının üretiminden sonra, metal-polimer hibrit yapının yarı statik mekanik performansı çekme-kesme testi ile açıklanmıştır. Sonrasında, kırılma yüzeylerinin morfolojisi taramalı elektron mikroskopisi (SEM) ile değerlendirilmiştir. Deneysel bulgular lazer ile işlenmiş yüzey dokusunun bu tür metal/polimer çoklu malzeme bağlantılarında mikro kenetleme yoluyla güçlü bağlantılar elde etmek için üstün bir aday olduğunun kanıtlandığını ortaya koymuştur. Nihai kuvvet 20 W lazer yüzey ön işleminden sonra 1515.10 N değerine ulaşmaktadır.

Anahtar Kelimeler: Tek bindirmeli bağlantılar, Sıcak presleme, Lazer ile uzaklaştırma işlemesi, Kırılma yüzeyi


1. Introduction

Competing demand of weight reduction results in a set of challenges for which the use of a combination of dissimilar parts can be a promising solution (Bilgin et al.

2019). Multi-material structures have emerged as a popular concept in order to benefit from the outstanding properties of different materials such as polymeric and metallic based materials (Dasilva et al. 2021). Dissimilar joints can lead to practical engineering solutions especially for automotive and aeronautical industries (Akpınar 2019). Compared with traditional connection methods such as mechanical fastening and welding, adhesion technology in the joining of adherends made of dissimilar materials has many advantages of cost effectiveness (Dantas et al. 2021), corrosion resistance (Gultekin 2022), design flexibility and ease of production

*Corresponding author: nahit.oztoprak@deu.edu.tr

Nahit Öztoprak  orcid.org/0000-0003-1132-8768

Gökçe Mehmet Gençer  orcid.org/0000-0003-1084-7240



(Huang et al. 2021). However, the joining through adhesive bonding process is facing significant drawbacks because of some adhesives that require heat curing (Agha and Abu-Farha 2021) and possible non-uniform stress distributions at the end of overlap area (Cetkin 2021). Therefore, direct bonding has received increasing attention in recent years due to especially its practicalness of time saving (Oztoprak 2021a). Hot-pressing joining can meet the growing requirements for adhesive-free adhesion without any additional components, and thus, has great potential with high-quality joints for its utilization in various engineering fields (Liu et al. 2021a, Oztoprak 2021b). Considering their convenience in fabrication and low cost (Kanani et al. 2020), single-lap joints (SLJs) are considered as the outstanding candidates for the bonding of dissimilar adherends. Undoubtedly, there is a need for particular modification to the metal surface in dissimilar joints in order to increase the bond strength. Here, laser ablation treatment can be more suitable for the modification of metal surface topography (Zhang et al. 2021). Laser processing offers environmental friendliness and repeatability as well as effectuality (Min et al. 2020).

Up to now, a large number of studies have focused on the laser pre-treatment of Al alloys. Most of the researches are dealing with the adhesive bonding (Akman et al. 2021, Schanz et al. 2021, Feng et al. 2021). However, only limited work exists on the mechanical performance of metal/polymer joints manufactured by hot-pressing. Therefore, there is a need to better understand the fracture mechanism of dissimilar joints through adhesiveless bonding. Liu et al. (2020) investigate the different microstructural morphologies on the lap joint shear strength of CFRP/AA7075 with laser surface processing. The joint fabrication is performed by hot-pressing process. They have found that the line pattern and square wave structures enhance the sudden fracture and increase the failure displacement by comparison with the untreated lap joint. Liu et al. (2021b) perform a comprehensive experimental study on the CFRP/Ti6Al4V hot-pressing joints of laser treatment with various textured grid widths. Their results indicate that the shear force first increases and then declines with the increase of grid width from 0.1 mm to 0.4 mm. Interface failure and cohesive failure are observed as the main damage mechanisms. In addition, in the research reported by Zhou et al. (2021), ultrasonic vibration assisted hot pressing method is utilized for the fabrication of carbon fiber/AZ31 Mg-based (CF/Mg-based) hybrid laminates bonded with Mg-Zn-Al eutectic alloy solder. Mechanical

properties and failure mechanism of the laminates are evaluated in their study. The laminates bonded through the solder exhibit a superior interlaminar fracture toughness by comparison with the laminates bonded with epoxy resin. Considering the brief literature review, the previous studies have only focused on examining the dissimilar joints with carbon fiber-reinforced polymers. However, fundamental research on the tensile-shear properties and failure modes of the SLJs between glass fiber-reinforced thermoplastic composites and non-heat treatable aluminum/magnesium (Al/Mg) alloys is still limited. Herein, our main goal is to evaluate the bonding and failure mechanisms of the multi-material joint manufactured by hot pressing as the direct bonding process. 5754 Al alloy and 40 wt.% long glass fiber reinforced-polypropylene (PP) composite are used for the metallic and polymeric adherends, respectively. In this paper, 20 W laser treatment is studied for the surface texturing of AA5754 prior to the adhesiveless (adhesive-free) bonding. It is proved that the laser ablation treatment enhances the adhesion performance of the thermoplastic composite.

2. Experimental Procedures

2.1. Materials

The metallic and thermoplastic composite adherends used for the present research are 3.15 mm thick 5754-H1111 Al alloy sheet and 4 mm thick E-glass reinforced (40 wt.%) PP composite, respectively. The nominal chemical compositions and mechanical properties of AA5754 are listed in Table 1 and Table 2, respectively. The panel of composite adherend is fabricated by homopolypropylene composite granules using a hot-pressing technique. The granules are kept in the hot press (Fontijne Presses - LabEcon60 Laboratory Platen Press, The Netherlands) at the constant force of 100 kN and constant temperature of 210 °C to prepare the composite panel. The basic physical and mechanical properties of the thermoplastic composite given by the supplier are 1.20 g/cm³, 119 MPa and 190 MPa for the density, tensile and flexural strength, respectively.

2.2. Laser surface patterning

Laser texturing, which gives the opportunity of obtaining a unique surface pattern via preferential material melting and vaporizing, is carried out on AA5754-H1111 to prepare the joint interface of the composite-metal hybrid structure (Figure 1). A grid texture model is produced at the overlap region by using a pulsed fiber laser processing system (SCANLAB GmbH, München, Germany) with the maximum output power of 20 W. The laser beam works at

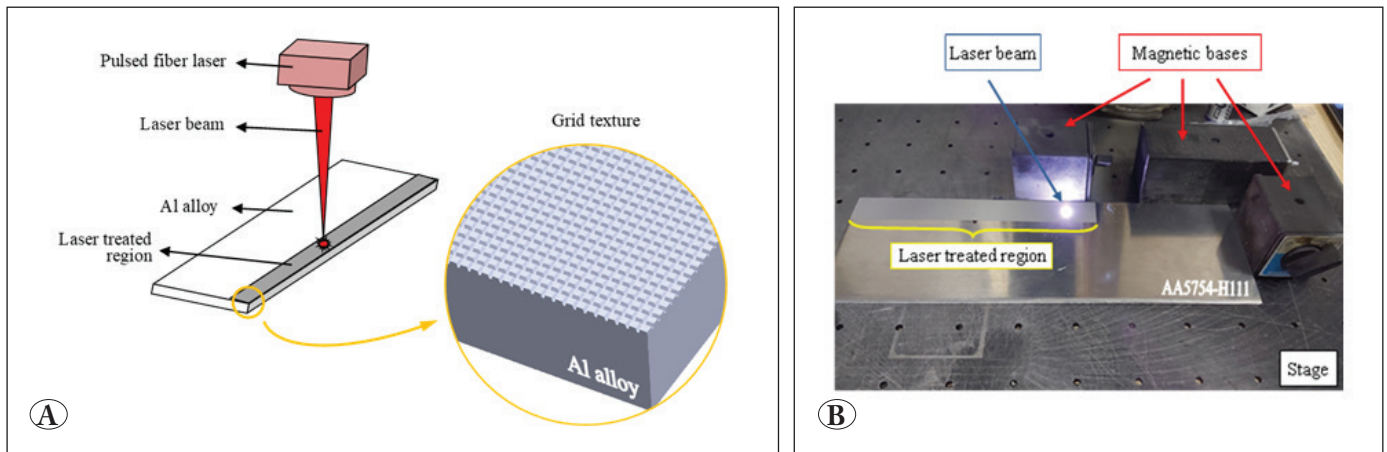


Figure 1. A) Schematic representation of the laser surface texturing, B) Processing of the AA5754-H111 surface.

Table 1. Chemical composition of 5754 Al alloy (wt.%).

Material	Mg	Mn	Fe	Si	Cr	Cu	Zn	Ti	Al
AA5754-H111	2.6-3.6	0.5	0.4	0.4	0.3	0.1	0.2	0.15	Balance

Table 2. Properties of the metallic adherend by the supplier.

Properties	AA5754-H111
Tensile strength (MPa)	190-240
Yield strength (MPa)	80
Elongation (50%)	18

the wavelength of 1064 nm and has a focal spot diameter of 32 μm . The laser surface texturing is performed in an open atmosphere. The laser beam is maintained perpendicular to the sample surface during the treatment and the focusing length is arranged as 215 mm. The laser processing parameters utilized for the irradiation of the surface of Al alloy substrate such as percentage of maximum power (η), scanning speed (v) and pulse frequency (f) are set as 100%, 300 mm/s and 25 kHz, respectively. The designed grid texture consists of equidistant grooves that have specific dimensions as a groove width of $\sim 200 \mu\text{m}$ and a centerline distance of $\sim 500 \mu\text{m}$ between adjacent grooves. Laser processing is carried out through eight consecutive scans with the same process parameters in order to allow adequate depth and thus, favorable micro interlocking between the polymer-Al alloy. Subsequently, in order to eliminate possible contaminants, surface cleaning is carried out through acetone and the metallic sheet is then dried with compressed air. After the surface modification of AA5754 substrate, 3D mapping of the laser ablation-treated region is also examined in an area of $2.5 \times 2.5 \text{ mm}^2$ via Ambios XP-2 Surface Profilometer.

The macrograph and micrograph investigations of the grid texture and joint interface are also performed. SEM and optical microscopy (OM) are utilized for the examinations.

2.3. Direct bonding process

Firstly, the surface-treated Al sheet is placed at the bottom of a mold with appropriate dimensions. The composite is then positioned on the metal surface to form the SLJ with the lap length of 25.4 mm. Hot-pressing joining of the PP composite is finally performed onto the AA5754 sheet through the hot press used in the fabrication of composite adherend at 210 $^{\circ}\text{C}$ and 100 kN force in the processing time of 50 min. Herein, polytetrafluoroethylene (PTFE) films are utilized between the adherends and metal press platens to prevent the melted PP sticking to the press. The schematic illustration and the details of hot-pressing process are shown in Figure 2.

2.4. Mechanical testing and fractographic examination

Tensile-shear properties of the SLJ are evaluated through the universal testing machine (Shimadzu AG-X) with a 100 kN load cell at a room temperature. The crosshead speed is set at 13 mm/min according to the procedure of ASTM D5868 (ASTM International 2014). Force-displacement data are provided by the test machine. Figure 3 demonstrates the SLJs investigated in this work. Fractured surfaces of the tensile-shear test specimens are scrutinized through the SEM (Thermo Scientific Apreo S) at 7.5 kV to have an insight of morphology and failure mechanism.

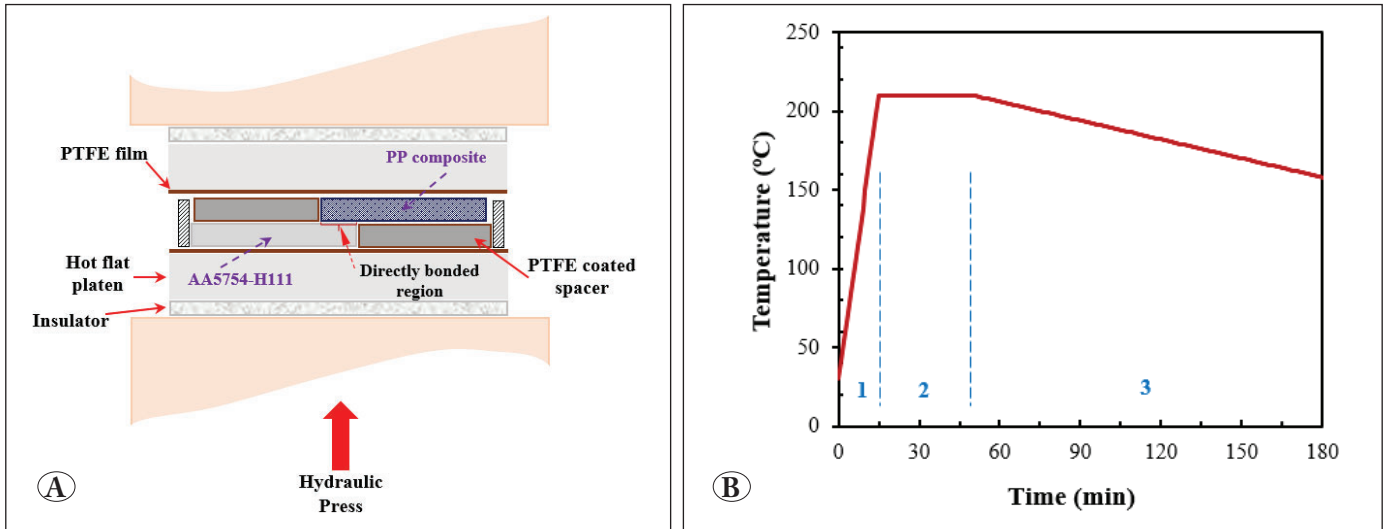


Figure 2. Hot-pressing process: A) Schematic diagram, B) Temperature curve.

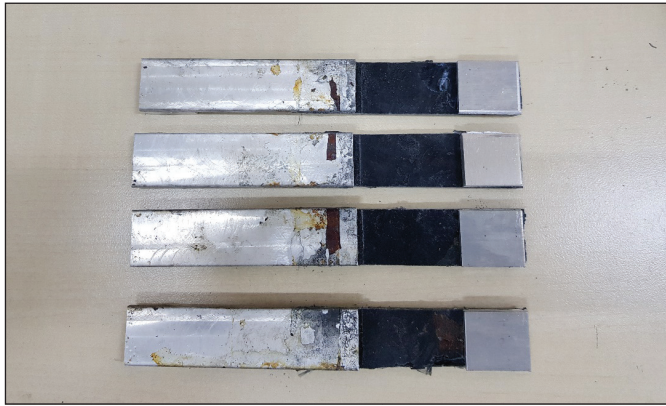


Figure 3. Tensile-shear test specimens.

The surfaces of the samples are sputter-coated with a thin layer of gold-palladium (Au-Pd) before the investigations. Fractured surfaces are inspected to observe signs of failure at the joint interface and at the composite adherend.

3. Results and Discussions

3.1. Laser ablation morphology and interface characterization

In the designs that two parts are directly joined to each other, surface preparation has an important role in obtaining favorable adhesion and joint strength (Maressa et al. 2015). Depending on the process parameters that exceed the specific threshold energy values for ablation of the metallic adherend, a controlled increase of the adhesion and mechanical interlocking area has been ensured during laser texturing (Akman et al. 2021). Figure 4 shows the surface macrography and morphology of the obtained texture on

the joint surface of the Al plate via laser ablation. It can be clearly seen from the surface macrography and morphology that a regular grid texture has been successfully fabricated on the joint surface. In the morphology findings, the yellow zones depict the unprocessed surface regions while the blue zones designate the bottom of the ablated grooves. The sharp-pointed red ridges refer to the cast structured micro burrs that formed around the processed zone due to the splashing and then rapid solidification of the melted material during the laser ablation. These micro splashes of the melted Al alloy have resulted in the formation of a complex morphology that significantly increases the adhesion area on the joint surface during the laser-generated texturing process (Figure 5). The cross-section of the joint interface (Figure 6) shows the profile and specific dimensions of the grid texture clearly. The mean widths of the unprocessed surface (top of the grid texture) and grooves with inclined surface geometry have been obtained as $273.7 \pm 4.8 \mu\text{m}$ and $211.7 \pm 4.4 \mu\text{m}$, respectively. The measured dimensions of the surface profile are in good agreement with the surface morphology results. The cross-section image also informs the wetting state at the interface and fiber distribution in the composite. A full wetting and penetration have been observed that point out the sufficient bonding between the thermoplastic composite and Al alloy. Irregular dispersion of the longitudinal and latitudinal sections of the fibers in Figure 6 indicates the random distribution of fibers in the composite structure. As in similar studies, the intense burr formation that enhances the surface roughness, micro interlocking, and thereby the joint strength of the directly bonded aluminum-composite hybrid structure is obvious

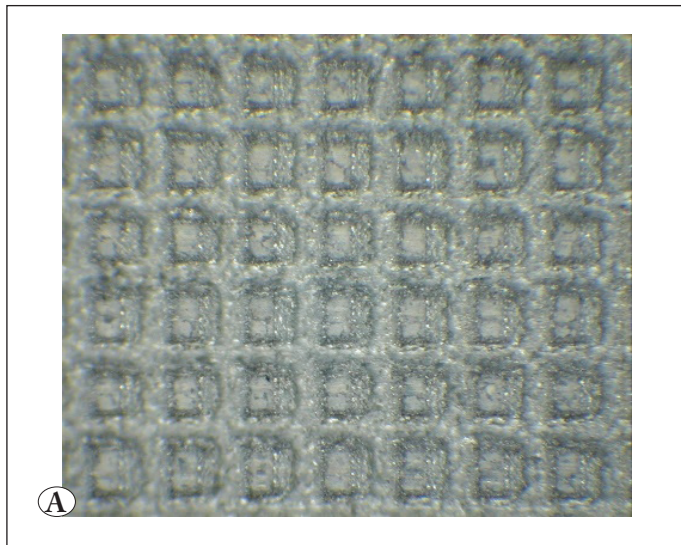
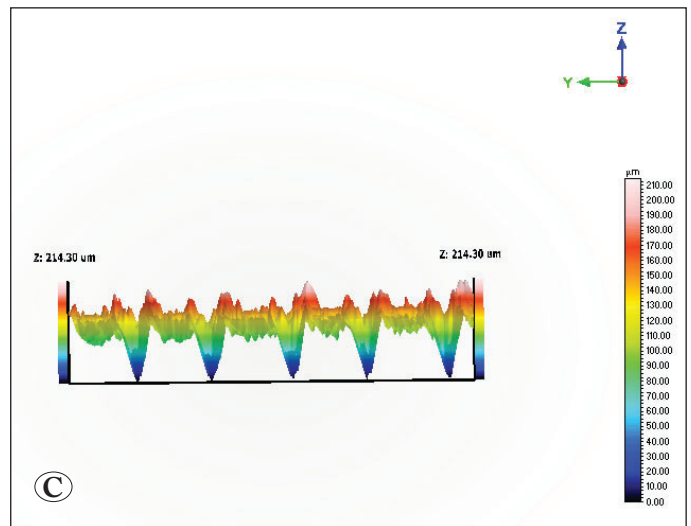
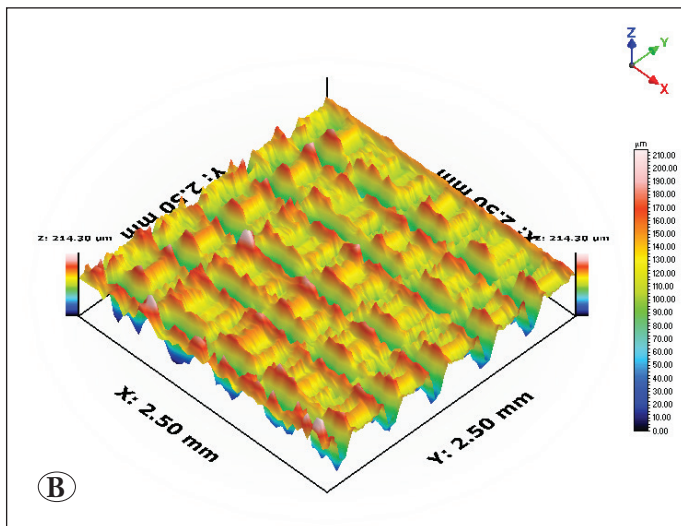


Figure 4. Macrostructure and 3D mapping images of the laser-treated surface: **A)** macrograph, **B)** isometric view, **C)** cross-section view.



on the grid-textured surface (Wu et al. 2016, Harris and Beevers 1999). It is noteworthy to mention that the laser ablation modifies the surface physicochemical properties of the Al alloy significantly (Wan et al. 2022). Besides obtaining a rough and complex-shaped surface, a thicker oxide layer is also generated on the Al surface by micro-scaled locally created high temperatures during the laser ablation (Al-Sayyad et al. 2019). Wu et al. (2016) stated that the oxide layer enhances the surface hydrophilicity of Al surfaces. Consequently, the laser-irradiation also makes an additional contribution to the improvement of the shear strength via enhancing the surface wetting properties which ensures a favorable microinterlocking at the bonding interface.

3.2. Tensile-shear properties

Figure 7 shows the experimental force-displacement curves obtained under quasi-static tensile loading. The average

maximum tensile force is noted as 1186.46 N. It can be obtained from the figure that two of the samples exhibit similar response as presented by the linear trend subsequent to the nonlinear increase at the initial response with the increase in displacement. The trend of these joints translates from non-linear to linear at the tensile displacement of about 1.3 mm. The linear behavior after initial recovery indicates that the joints behave elastically without a plastic process. After reaching the ultimate tensile force, brittle fracture with a rich sound is reported. The failure mode of these two samples is mainly included as fiber tear failure with a large amount of fibers remaining on the Al sheet. Failure position after the tensile-shear testing is also exhibited in Figure 8. Considering the specimens failed from the composite adherend (Sample_2 and Sample_3 in Figure 7), it can be clearly seen that there is a larger extension rather than a sudden load drop after the maximum level. It is noteworthy

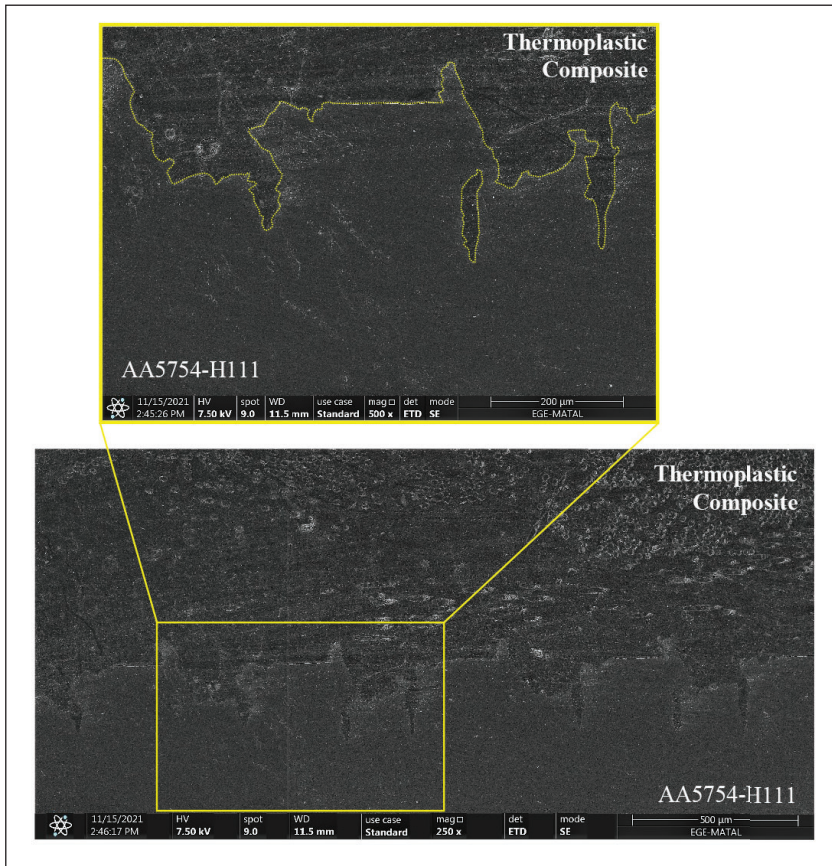


Figure 5. SEM image of the complex surface profile at the joint interface.

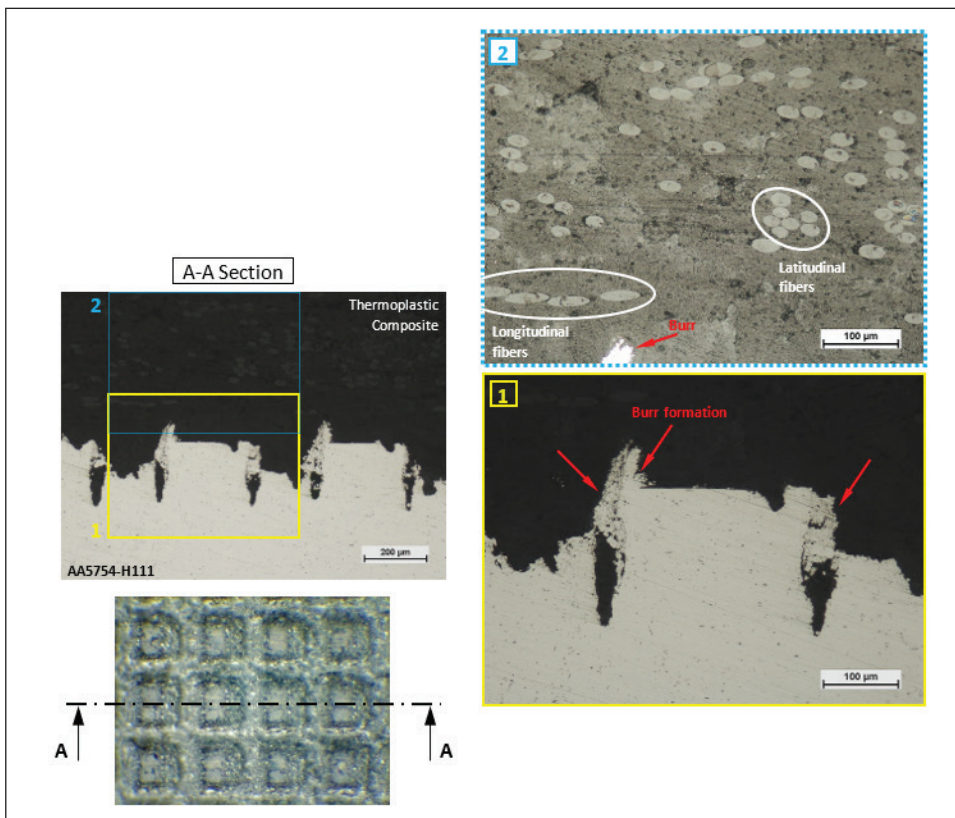


Figure 6. Optical micrograph of the joint cross-section.

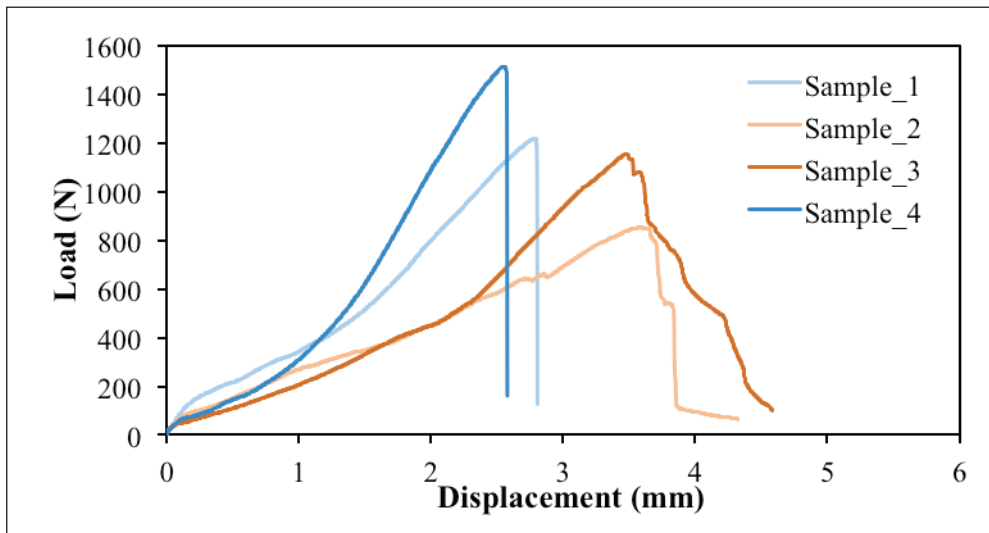


Figure 7. Response curves of SLJs under tensile loading.

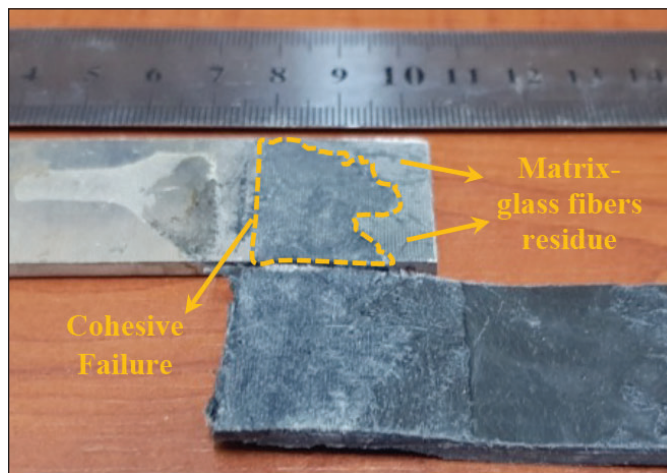


Figure 8. Failure position and surface appearance of SLJs.

that the failure elongation is evidently greater as the damage in the polymeric material allows the composite to deformation (Oztoprak 2021a). The other point that should be considered here is the thermal cycle applied during the direct bonding process, but even if the situation in question may be effective, the absence of interface damage at the measured load values is very important in terms of evaluating the joint strength.

3.3. Failure mechanisms

To get insight into the failure modes of the dissimilar joints, fracture surfaces of the samples after tensile-shear testing are evaluated. Figure 9 and Figure 10 exhibit the SEM observations on the metallic adherend of the specimen failed at the joint interface. As can be seen in Figure 9, the polymer fills all grooves, although the surface locally shows a cleaner

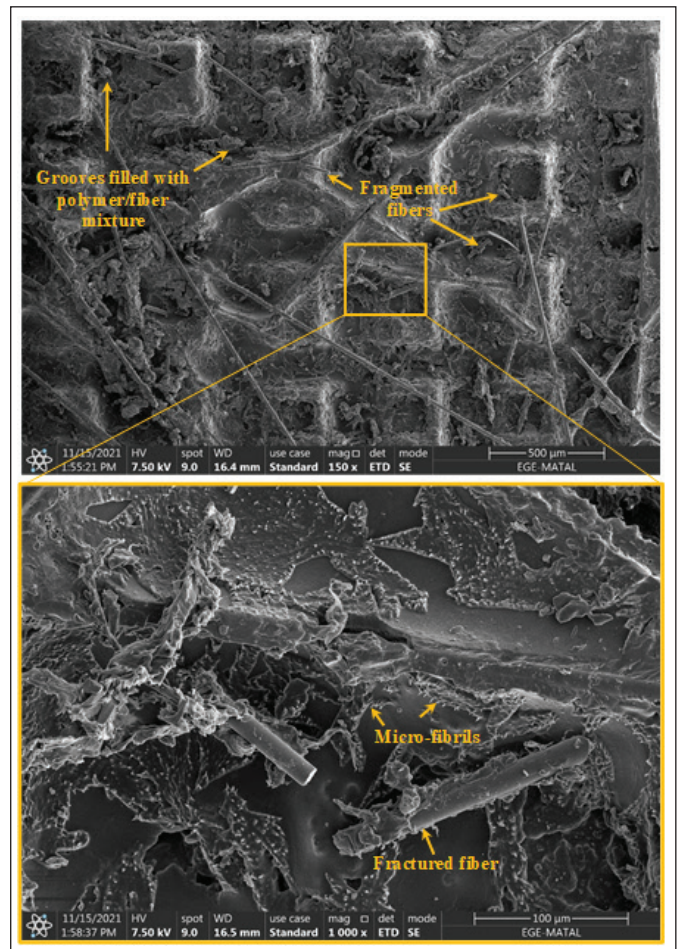


Figure 9. SEM images of the joint interface at the 5754 Al with polymer-fibers residue.

metal surface than other regions. Additionally, fractured fibers and micro-fibrils in the polymer draw the attention. Except for this region, which takes place in a smaller area, cohesive failure is observed. Considering Figure 10, the surface undergoes fiber/matrix debonding in addition to the fragmented fibers. Herein, it has been realized that the debonding of the fibers is not smooth, the cohesive matrix confirms the strong adhesion. Similar to the metal surface, the morphology on the composite presents the fiber fracture and debonding (Figure 11). Fragmented fibers are the dominant failure indication on the surface as shown in Figure 12. On the other hand, the fracture mechanism of the joint changes from fiber fracture to pulled-out fibers for the specimens failed from the PP composite (Figure 13), which leads to decrease in the ultimate force to failure. Poor fiber/matrix adhesion in the sample with smooth fiber surfaces results in fracture easily and rough structure of the polymer confirms the ductile fracture of the sample.

4. Conclusions

In this study, fracture surface observation of the AA5754-PP composite assembly subjected to tensile-shear loading is performed. To provide mechanical micro-interlocking, laser micro-structure with grid texture is fabricated on the metal adherend. Bonding strength of the SLJ is experimentally evaluated. The main findings of the work are as follows:

1. After the laser surface texturing, an intense re-cast micro burr formation is observed on the laser-treated region that increases the surface roughness through the formation of a complex morphology with the micro splashes of the melted Al alloy, thereby the joint strength.
2. Full penetration of the thermoplastic composite in the laser-etched grooves is reported that results in obtaining a favorable bonding.
3. Under quasi-static tensile loading, the samples are fractured from two different regions (interface and

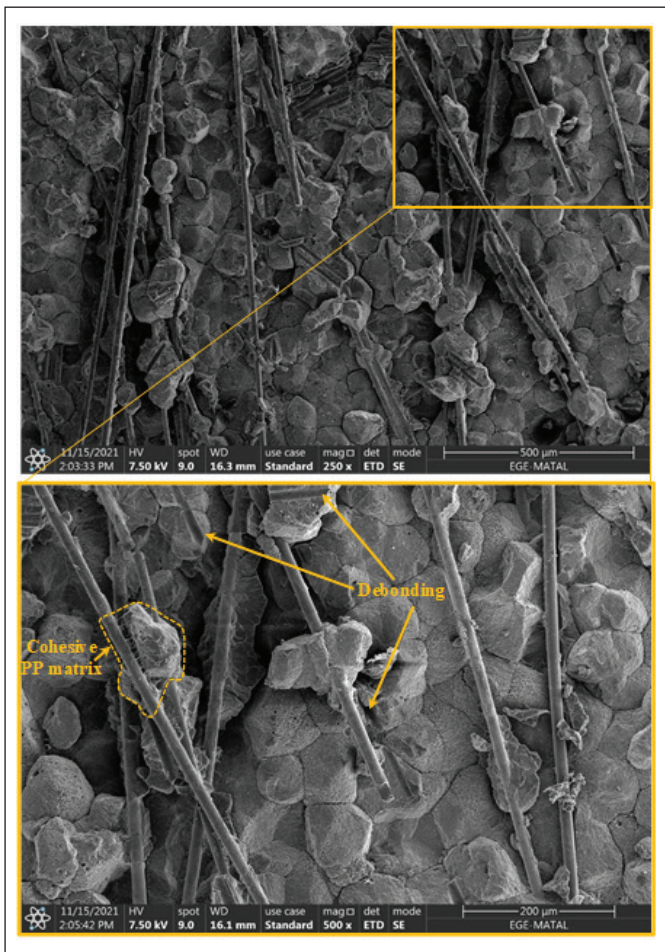


Figure 10. SEM images of the joint interface at the 5754 Al with cohesive failure.

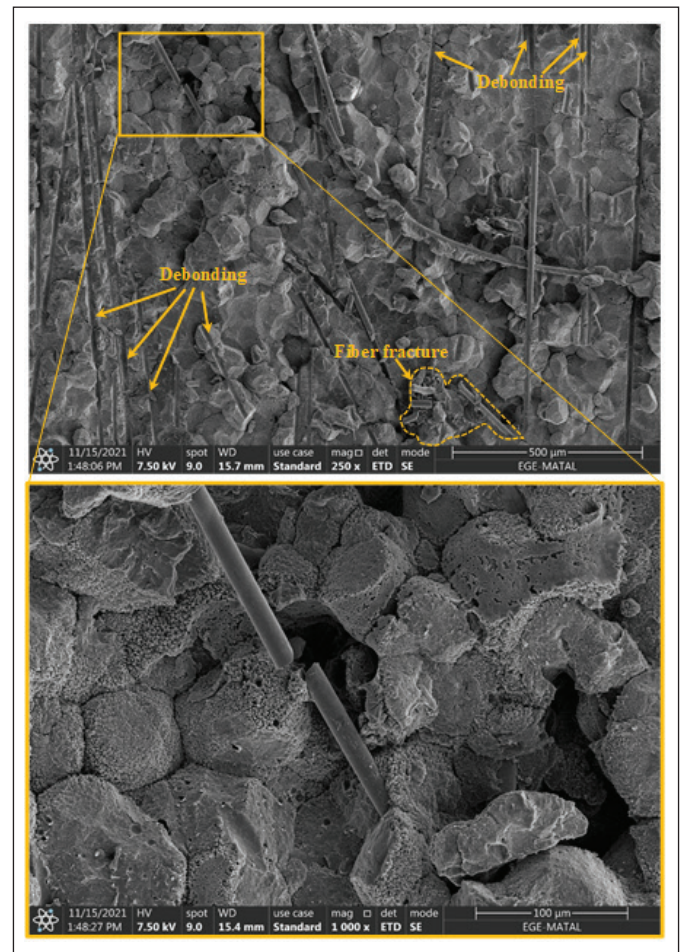


Figure 11. SEM images of the joint interface at the composite adherend with strong bonding.

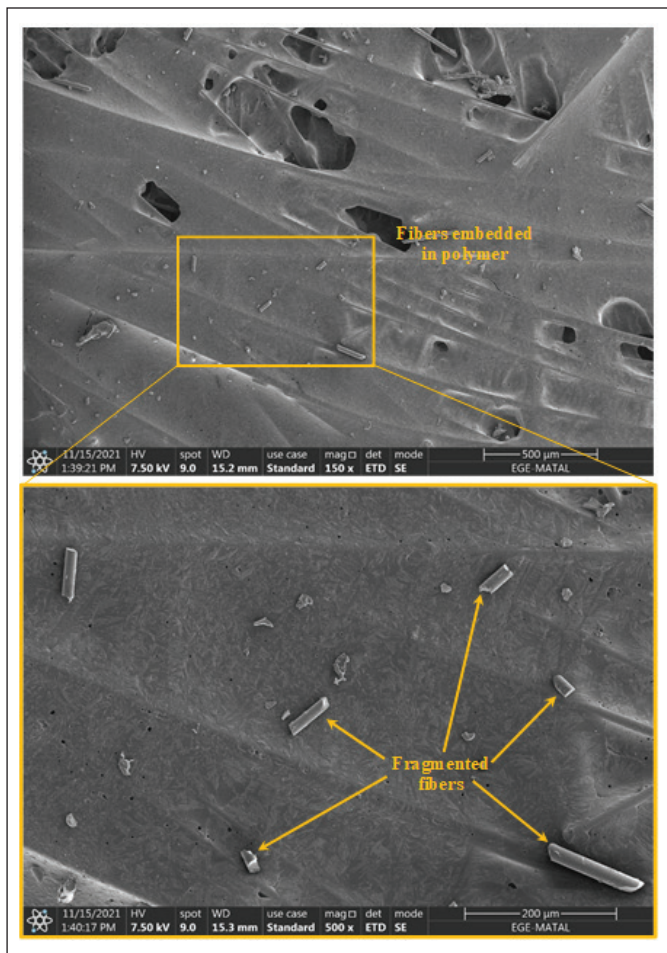


Figure 12. SEM images of the joint interface at the composite adherend with smoother fracture surface.

composite adherend). 1186.46 N is calculated as the average maximum tensile force of the hybrid GFRT-P-Al alloy joint.

- Fractography evidences that the fracture mechanisms of the samples, which fail from the joint interface and the composite adherend, are fiber fracture and fiber pull out, respectively.

Acknowledgments

Thanks to Seykoç Aluminum and Nuh Kompozit for their support in the supply of the metallic adherend and composite granules, respectively.

Conflict of Interest

The authors declare that they have no known competing financial interests or personal relationships that could have appeared to influence the work reported in this paper.

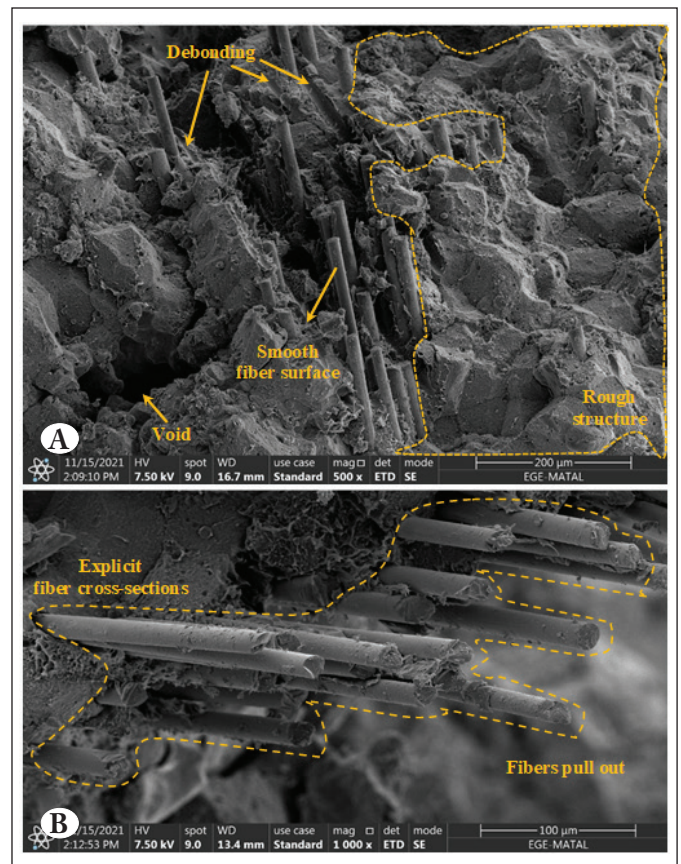


Figure 13. SEM images of the composite adherend in different magnifications: **A)** 500x, **B)** 1000x.

5. References

- Agha, A., Abu-Farha, F. 2021. Viscoelastic model to capture residual stresses in heat cured dissimilar adhesive bonded joints. *International Journal of Adhesion and Adhesives*, 107: 102844. <https://doi.org/10.1016/j.ijadhadh.2021.102844>
- Akman, E., Bora, M. Ö., Çoban, O., Öztoprak, B. G. 2021. Laser-induced groove optimization for Al/CFRP adhesive joint strength. *International Journal of Adhesion and Adhesives*, 107: 102830. <https://doi.org/10.1016/j.ijadhadh.2021.102830>
- Akpınar, S. 2019. The Effect of Adherend Thickness and Width on Fracture Behavior in Adhesively bonded Double Cantilever Beam Joints. *European Mechanical Science*, 3(3): 83-87. <https://doi.org/10.26701/ems.566773>
- Al-Sayyad, A., Bardon, J., Hirchenhahn, P., Vaudémont, R., Houssiau, L., Plapper, P. 2019. Influence of Aluminum Laser Ablation on Interfacial Thermal Transfer and Joint Quality of Laser Welded Aluminum-Polyamide Assemblies. *Coatings*, 9: 768. <https://doi.org/10.3390/coatings9110768>
- ASTM International. 2014. Standard test method for lap shear adhesion for fiber reinforced plastic (FRP) bonding, ASTM D5868-01(2014), ASTM International Standards, West Conshohocken.

- Bilgin, M., Karabulut, Ş., Özdemir, A. 2019.** Effect of preheating and dry ice cooling on dissimilar friction stir welding of AA7075-T6 and AZ31B. *Journal of Polytechnic*, 22(3): 655-663. <https://doi.org/10.2339/politeknik.426649>
- Cetkin, E. 2021.** Investigation of the Effects of Use of GNP and GNP Reinforced Nano-Fibers with Epoxy Adhesive on Tension Tests. *European Journal of Technique*, 11(2): 175-181. <https://doi.org/10.36222/ejt.957654>
- Dantas, M. A., Carbas, R. J. C., Marques, E. A. S., Kushner, D., da Silva, L. F. M. 2021.** Flexible tubular metal-polymer adhesive joints under torsion loading. *International Journal of Adhesion and Adhesives*, 105: 102787. <https://doi.org/10.1016/j.ijadhadh.2020.102787>
- Dasilva, S., Jimenez-Suarez, A., Rodriguez, E., Prolongo, S. G. 2021.** Quality assessment and structural health monitoring of CNT reinforced CFRP and Ti6Al4V multi-material joints. *Materials & Design*, 210: 110118. <https://doi.org/10.1016/j.matdes.2021.110118>
- Feng, Z., Zhao, H., Tan, C., Zhang, X., Chen, B., Song, X. 2021.** Nanosecond laser ablation for improving the strength of CFRTP and aluminum alloy adhesively bonded joints. *Composite Structures*, 274: 114369. <https://doi.org/10.1016/j.compstruct.2021.114369>
- Gultekin, K. 2022.** Comparison of the effect of modified and unmodified boron carbide (B₄C) nanoparticles on the mechanical properties of structural adhesives. *Niğde Ömer Halisdemir University Journal of Engineering Sciences*, 11(1): 198-206. <https://doi.org/10.28948/ngumuh.984658>
- Harris, A.F., Beevers, A. 1999.** The effects of grit-blasting on surface properties for adhesion". *International Journal of Adhesion & Adhesives*, 19: 445-452. [https://doi.org/10.1016/S0143-7496\(98\)00061-X](https://doi.org/10.1016/S0143-7496(98)00061-X)
- Huang, W., Sun, L., Liu, Y., Chu, Y., Wang, J. 2021.** Effects of low-energy impact at different temperatures on residual properties of adhesively bonded single-lap joints with composites substrate. *Composite Structures*, 267: 113860. <https://doi.org/10.1016/j.compstruct.2021.113860>
- Kanani, A. Y., Hou, X., Ye, J. 2020.** The influence of notching and mixed-adhesives at the bonding area on the strength and stress distribution of dissimilar single-lap joints. *Composite Structures*, 241: 112136. <https://doi.org/10.1016/j.compstruct.2020.112136>
- Liu, X., Zhu, H., Xie, Y., Xu, L., Lin, N., Lu, L. 2020.** Optimization of microstructural morphology via laser processing to enhance the bond strength Al-CFRP. *Journal of Reinforced Plastics & Composites*, 40(11-12): 463-473. <https://doi.org/10.1177/0731684420973066>
- Liu, Y., Su, J., Ma, G., Han, X., Tan, C., Wu, L., Chen, B., Song, X. 2021a.** Effect of the laser texturing width on hot-pressing joining of AZ31B and CFRTP. *Optics & Laser Technology*, 143: 107350. <https://doi.org/10.1016/j.optlastec.2021.107350>
- Liu, Y., Su, J., Tan, C., Feng, Z., Zhang, H., Wu, L., Chen, B., Song, X. 2021b.** Effect of laser texturing on mechanical strength and microstructural properties of hot-pressing joining of carbon fiber reinforced plastic to Ti6Al4V. *Journal of Manufacturing Processes*, 65: 30-41. <https://doi.org/10.1016/j.jmapro.2021.03.021>
- Maressa, P., Anodio, L., Bernasconi, A., Demir, A.G., Previtali, B. 2015.** Effect of surface texture on the adhesion performance of laser treated Ti6Al4V alloy. *The Journal of Adhesion*, 91(7): 518-537. <https://doi.org/10.1080/00218464.2014.933809>
- Min, J., Wan, H., Carlson, B. E., Lin, J., Sun, C. 2020.** Application of laser ablation in adhesive bonding of metallic materials: A review. *Optics & Laser Technology*, 128: 106188. <https://doi.org/10.1016/j.optlastec.2020.106188>
- Oztoprak, N. 2021a.** Directly bonded single lap joints of SiCp/AA2124 composite with glass fiber-reinforced polypropylene: Hole drilling effects on lap shear strength and out-of-plane impact response. *Journal of Composite Materials*, 55(20): 4045-4061. <https://doi.org/10.1177/00219983211031648>
- Oztoprak, N. 2021b.** Investigation of metal-matrix composite based hybrid laminates under quasi-static penetration and Charpy impact loading. *Journal of Manufacturing Processes*, 68(A): 1328-1338. <https://doi.org/10.1016/j.jmapro.2021.06.063>
- Schanz, J., Meinhard, D., Dostal, I., Riegel, H., De Silva, A. K. M., Harrison, D. K., Knoblauch, V. 2022.** Comprehensive study on the influence of different pretreatment methods and structural adhesives on the shear strength of hybrid CFRP/aluminum joints. *The Journal of Adhesion*, 98(12): 1772-1800. <https://doi.org/10.1080/00218464.2021.1938004>
- Wan, H., Min, J., Lin, J. 2022.** Experimental and theoretical studies on laser treatment strategies for improving shear bonding strength of structural adhesive joints with cast aluminum. *Composite Structures*, 279: 114831. <https://doi.org/10.1016/j.compstruct.2021.114831>
- Wu, Y., Lin, J., Carlson, B.E., Lu, P., Balogh, M. P., Irish, N.P., Mei, Y. 2016.** Effect of laser ablation surface treatment on performance of adhesive-bonded aluminum alloys. *Surface & Coatings Technology*, 304: 340-347. <https://doi.org/10.1016/j.surfcoat.2016.04.051>
- Zhang, C., Chen, L., Zhang, Y., Wang, G., Jin, J. 2021.** Effect of laser processing microstructure on the bonding strength and failure mode of 7075-T6 aluminum alloy adhesive joints. *Journal of Manufacturing Processes*, 66: 302-312. <https://doi.org/10.1016/j.jmapro.2021.04.028>
- Zhou, X., Zhao, Y., Chen, X., Liu, Z., Li, J., Fan, Y. 2021.** Fabrication and mechanical properties of novel CFRP/Mg alloy hybrid laminates with enhanced interface adhesion. *Materials & Design*, 197: 109251. <https://doi.org/10.1016/j.matdes.2020.109251>